Journal of Luminescence 152 (2014) 133–137

Contents lists available at ScienceDirect

Journal of Luminescence

journal homepage: www.elsevier.com/locate/jlumin

Photoluminescence characteristics of Sm^{3+}-doped Ba_2CaWO_6 as new orange–red emitting phosphors

Ruijn Yu [a,b,c], Hyeon Mi Noh [b], Byung Kee Moon [b], Byung Chun Choi [b], Jung Hyun Jeong [b,*], Ho Sueb Lee [c], Kiwan Jang [c,**], Soung Soo Yi [d]

[a] College of Science, Northwest A&F University, Yangling, Shaanxi 712100, PR China
[b] Department of Physics, Pukyong National University, Busan 608-737, Republic of Korea
[c] Department of Physics, Changwon National University, Changwon 641-773, Republic of Korea
[d] Department of Electronic Material Engineering, Silla University, Busan 617-736, Republic of Korea

ARTICLE INFO

Available online 11 February 2014

Keywords:
Luminescence
Ba_2CaWO_6:Sm^{3+}
Phosphor
Tungstate

ABSTRACT

The orange–red emitting Ba_2CaWO_6:$x$$Sm^{3+}$ ($0.01 \leq x \leq 0.25$) phosphors were synthesized via solid state reaction process. The crystal structure of the phosphor was characterized by XRD. The photoluminescence excitation and emission spectra, concentration effect were investigated. The results show an efficient energy transfer from WO_6^{6-} group to Sm^{3+} occurs. The emission spectra of the Ba_2CaWO_6:Sm^{3+} phosphors consisted of some sharp emission peaks of Sm^{3+} ions centre at 579 nm, 618 nm, 625 nm, and 675 nm. The strongest one is located at 610 nm due to $^4G_{5/2} \rightarrow {}^6H_{7/2}$ transition of Sm^{3+}, generating bright orange–red light. The optimum dopant concentration of Sm^{3+} ions in Ba_2CaWO_6:$x$$Sm^{3+}$ is around 5 mol % and the critical transfer distance of Sm^{3+} is calculated as 18 Å. The fluorescence lifetime of Sm^{3+} in Ba_2CaWO_6:$0.05Sm^{3+}$ is 2.36 ms. The Ba_2CaWO_6:Sm^{3+} phosphors may be potentially used as orange–red phosphors for white light-emitting diodes.

1. Introduction

Inorganic luminescent materials have practical applications in almost all devices for artificial light production, especially in white light-emitting diodes (LEDs) illumination. Phosphor-converted white light-emitting diodes (PC-WLEDs) are the crucial developments of solid-state lighting, high efficiency and environmental safety [1–3]. To date, the most popular commercial PC-WLED is combination of a blue LED with a yellow phosphor. This type of white light has poor color render index (CRI) caused by the absence of red composition. It is also possible to use nitride phosphor blends to improve the CRI of PC-WLEDs. While nitride phosphors have the drawback of a relatively high manufacturing expense due to the severe synthesis conditions and high patent licensing costs. These problems can be resolved through the fabrication of WLEDs with tricolor (red, green, and blue) phosphors excited by a near-ultraviolet (UV) InGaN chips [4–7]. However, the commercially applicable red phosphor of Y_2O_2S:Eu^{3+} is chemically unstable (releasing of hydrogen sulfide gas) and its fluorescent efficiency is lower than that of the blue ($BaMgAl_{10}O_{17}$:Eu^{2+}) and green-emitting (ZnS:Cu^+, Al^{3+}) phosphors. Therefore, the investigations of new efficient red phosphors for W-LEDs have gained much attention.

It has been reported that $Mo(W)O_4$–$Mo(W)O_6$ groups can absorb near-UV and violet light efficiently [8,9]. Compared with the W(Mo) O_4 groups, the octahedral-coordinated $W(Mo)O_6$ groups could efficiently absorb violet light and transfer the excitation energy to the activator [10]. Recently, a series of host sensitized, Eu^{3+} ion-activated double perovskite system $A_2^{II}B^{II}M^{VI}O_6$ (A_2BMO_6):Eu^{3+} (A=Ba, Sr; B=Ca; M=Mo and W) phosphors were investigated [11–15]. These molybdate and tungstate phosphors have an efficient absorption band covering the wide ultraviolet range and extending to visible light range (200–450 nm), which mainly arises from the charge transfer (CT) transition of $Mo(W)O_6$ groups. The emission intensity of Eu^{3+}-doped Sr_2CaMoO_6 is 1.5 times higher than that of commercial Y_2O_2S:Eu^{3+} [11], and Eu^{3+}-doped $Sr_2Ca(Mo,W)O_6$ also shows a more luminescence intensity than the commercial Y_2O_2S:Eu^{3+} under 395 nm excitation [14]. Our group [16] recently investigated the photoluminescence properties of the analogue Ba_2MgXO_6:Eu (X=W and Mo) and the energy transfer from W $(Mo)O_6$ groups to Eu^{3+} ions within the phosphors. The $MoO_6 \rightarrow Eu^{3+}$ energy transfer efficiency could be greatly enhanced by partial substitution of Mo by W. These phosphors showed excellent color-conversion capability from near-UV to orange–red light. Compared

---

[*] Corresponding author. Tel.: +82 51 629 6285; fax: +82 51 629 5549.
[**] Corresponding author.
E-mail addresses: jhjeong@pknu.ac.kr (J. Hyun Jeong), kwjang@changwon.ac.kr (K. Jang).

http://dx.doi.org/10.1016/j.jlumin.2014.01.074
0022-2313

with Eu^{3+}, Sm^{3+} is an essential activator for many different inorganic lattices to produce orange–red emission because of its $^4G_{5/2} \rightarrow {}^6H_J$ ($J=5/2$, 7/2, 9/2, and 11/2) transitions. For example, new red- or orange–red-emitting phosphors doped with Eu^{3+} ion or/and Sm^{3+} have been developed, including Gd_2MoO_6:Sm^{3+}, $CaWO_4$:Sm^{3+} [17,18], Sm^{3+}-doped vanadate [19,20], M_2SiO_4:Sm^{3+}(M=Ba, Sr, Ca) [21], $Y_2Si_4N_6C$:Sm^{3+} [22], $KZnGd(PO_4)_2$:Eu^{3+}, Sm^{3+} [23].

We noticed that the cubic double-perovskite structure Ba_2CaWO_6 have not been investigated as the Sm^{3+}-activated host lattice. For understanding the wide range excitations and the energy transfers from WO_6 to Sm^{3+}, we investigated the photoluminescence properties of Ba_2CaWO_6:Sm^{3+} phosphors.

2. Experimental

A series of powder samples of $Ba_2Ca_{1-x}WO_6$:xSm^{3+} ($x=0.01$, 0.03, 0.05, 0.08, 0.10, 0.15, and 0.20) was synthesized by a high-temperature solid-state reaction. The starting materials $BaCO_3$ (>99%), $CaCO_3$ (>99%), WO_3 (99.0%), and Sm_2O_3 (99.99%) obtained from Sigma-Aldrich were thoroughly mixed and ground in an agate mortar. The mixture was preheated at 850 °C for 24 h in a muffle furnace, reground, and finally fired at 1200 °C for 12 h in air. After reaction at 1200 °C, the products were slowly cooled down to room temperature by switching off the muffle furnace and then ground into powder. The whole process involves the following solid-state reaction

$$2BaCO_3 + (1-x)CaCO_3 + WO_3 + (x/2)Sm_2O_3 \xrightarrow{850\ ^\circ C,\ 24\ h;\ 1200\ ^\circ C, 12\ h} Ba_2Ca_{1-x}Sm_xWO_6$$

The phase structure of the powders was examined by X-ray diffraction (XRD) on a Philips X'Pert MPD X-ray diffractometer (Philips, Netherlands) at 40 kV and 30 mA. The diffraction patterns were scanned within an angular range of 10°–60° (2θ) with a scan rate of 0.02°/s. The morphology and size of the phosphor particle were characterized using a scanning electron microscopy (SEM) system JSM-6490, JEOL Company. The sizes of as-prepared phosphors were estimated from laser particle size analyzer (Beckman Coulter LS13 320) by liquid state mode. The PL and PLE spectra were recorded on a Photon Technology International (PTI, USA) fluorimeter with a 60 W Xe-arc lamp. The temperature-dependent PL spectra of the phosphor were recorded in air on an Edinburgh FLS 920 spectrometer equipped with a 450 W Xe lamp. The PL decay of Sm^{3+} of the phosphor was measured using the third harmonic (355 nm) of a pulsed Nd:YAG laser (5 ns, 10 Hz).

3. Results and discussion

Alkaline earth molybdates and tungstates of the type A_2BMO_6 (A=Ba, Sr; B=Ca; M=Mo and W) crystallize in an ordered perovskite structure related to $(NH_4)_3FeF_6$ and cryolite, where the B and M atoms are ordered in alternate {1 1 1} cation layers. The crystal structure diagram of double perovskite Ba_2CaWO_6 was plotted using a version of diamond (3.2) software (Fig. 1). Structurally, the compound Ba_2CaWO_6 has a cubic unit cell ($a=8.392$ Å) with space group $Fm\overline{3}m$ (no. 225) [24]. The Ba^{2+} ions are coordinated by twelve oxygen atoms, and both Ca^{2+} and W^{6+} ions are six-fold coordinated to oxygen forming CaO_6 and WO_6 octahedra. These octahedra appear alternately in the cell and are connected with each other by sharing vertex oxygen [25].

The as-prepared Ba_2CaWO_6:Sm^{3+} sample was characterized by X-ray diffraction (XRD) patterns to verify the phase purity. As indicated in Fig. 2, we have observed that the doped Sm^{3+} ions have no obvious influence on the structure of the host, and all the diffraction peaks of the samples can be indexed to the cubic double perovskite structure Ba_2CaWO_6 (JCPDS 54-0188). The lattice constants of Ba_2CaWO_6 ($x=0.05$) are calculated to be $a=8.353$ Å, $V=582.81$ Å^3, which are consistent with the literature [24]. As the ionic radius of Sm^{3+} ($r=0.958$ Å, $CN=6$) is the closest to that of Ca^{2+} ($r=1.00$ Å, $CN=6$), compared with Ba^{2+} ($r=1.61$ Å, $CN=12$) and W^{6+} ($r=0.60$ Å, $CN=6$) [26], the doped Sm^{3+} is supposed to occupy the Ca^{2+} site. On the other side, similar to the Eu^{3+} lattice occupation in the Eu^{3+}-doped A_2BMO_6 [13,14,27], when Sm^{3+} was doped into the double perovskite structure, it was considered to preferably occupy B-site, namely, Ca^{2+}-site in Ba_2CaWO_6. In this case, W–O–Sm^{3+} is close to 180° and collinear, thus WO_6 groups can efficiently transfer their absorbed energy to Sm^{3+}.

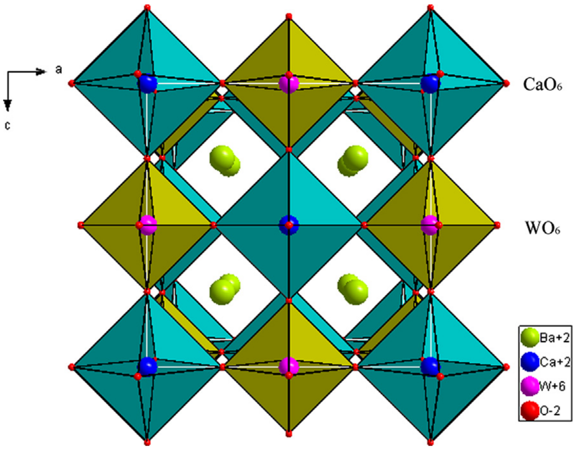

Fig. 1. The crystal structure of Ba_2CaWO_6. *Note:* Ba^{2+} cations are shown in green, and O^{2-} anions are shown in red. CaO_6 octahedra are shown in turquoise, and WO_6 octahedra are shown in yellow. (For interpretation of the references to color in this figure legend, the reader is referred to the web version of this article.)

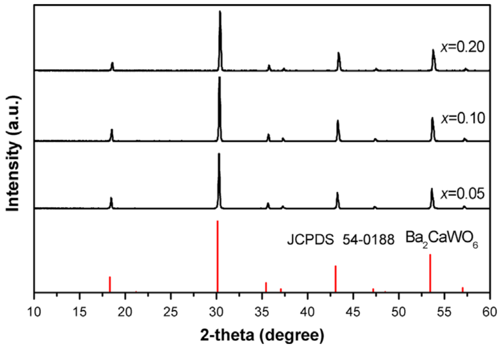

Fig. 2. XRD patterns of three representative Ba_2CaWO_6:xSm^{3+} samples ($x=0.05$, 0.10, and 0.20).

SEM analysis was carried out to investigate the surface morphology and particle sizes of the synthesized phosphor powder. Fig. 3 shows the representative SEM images of two different concentrations of Ba_2CaWO_6:xSm^{3+} (a, $x=0.05$; b, $x=0.15$). Both products mainly consisted of solid microcrystalline structures with some conglomeration among the crystalline grains for the high temperature solid-state reaction. Meanwhile, the particle sizes vary from few microns to several tens of microns. The as-prepared particles were dispersed into D.I water, and particle size was measured by Particle Size Analyzer (PSA) using Fraunhofer method. As can be seen from the insets of Fig. 3, the mean diameter of Ba_2CaWO_6:xSm^{3+} ($x=0.05$ and 0.15) was 24.65 μm and 35.24 μm, respectively, which was similar to diameter estimated from SEM image analysis. The morphologies of Ba_2CaWO_6:Sm^{3+} powders increase a little for the doping concentration from 0.05 mol% to 0.15 mol%. Most commercial phosphor particles currently available on the market are in a size range of 2–10 μm.